

Gaussian Processes-BayesFilters with Non-Parametric Data Optimization for Efficient 2D LiDAR Based People Tracking

Zulkarnain Zainudin ^{a,1,*}, Sarath Kodagoda ^{b,2}

^a Faculty of Electronics and Computer Engineering Technology, Universiti Teknikal Malaysia Melaka (UTeM), Hang Tuah Jaya, 76100 Durian Tunggal, Melaka, Malaysia

^b Centre for Autonomous Systems (CAS), Faculty of Engineering and Information Technology, University of Technology Sydney, PO Box 123 Broadway, Ultimo, NSW 2007, Australia

¹ zul@utem.edu.my; ² Sarath.Kodagoda@uts.edu.au

* Corresponding Author

ARTICLE INFO

Article History

Received January 18, 2023

Revised March 16, 2023

Accepted March 26, 2023

Keywords

People Tracking;

Gaussian Processes;

Bayesian Filter;

Particle Filter;

Extended Kalman Filter

ABSTRACT

A model for expressing and describing human motion patterns must be able to improve tracking accuracy. However, Conventional Bayesian Filters such as Kalman Filter (KF) and Particle Filter (PF) are vulnerable to failure when dealing with highly maneuverable targets and long-term occlusions. Gaussian Processes (GP) is then used to adapt human motion patterns and integrate the model with Bayesian Filters. In GP, all samples in training phase need to be included and periodically, new samples will be added into training samples whenever it is available. Larger amount of data will increase the computational time to produce the learned GP models due to data redundancies. As a result, Mutual Information (MI) based technique with Mahalanobis Distance (MD) is developed to keep only the informative data. This method is used to process data which is collected by a robot equipped with a LiDAR. Experiments have demonstrated that reducing data does not raise Average Root Mean Square Error (ARMSE) considerably. EKF, PF, GP-EKF and GP-PF are utilised as a tool for tracking people and all techniques have been analyzed in order to distinguish which method is more efficient. The performance of GP-EKF and GP-PF are then compared to EKF and PF where it proved that GP-BayesFilters performs better than Conventional Bayesian Filters. The proposed approach has reduced data points up to more than 90% while keeping the ARMSE within acceptable limits. This data optimization technique will save computational time especially when deal with periodically accumulative data sets. Comparing on four tracking methods, both GP-PF and GP-EKF have achieved higher tracking performance when dealing with highly maneuverable targets and occlusions.

This is an open access article under the [CC-BY-SA](https://creativecommons.org/licenses/by-sa/4.0/) license.



1. Introduction

Many academics are interested in exploring further applications in the fields of security, surveillance, and human-robot interaction by tracking objects in a dispersed setting [1, 2, 3, 4, 5, 6, 7, 8, 9]. Many studies have been carried out employing sensors including laser detection and ranging (LiDAR) [10, 11, 12, 13, 14, 15, 16] and camera, in various people detection and tracking systems. It is proven that light variations such as darkness and light do not affect LiDAR efficiency on measurements

[17, 18].

State estimation and data association are two fundamental techniques that being associated with Bayesian Filters such as the Kalman Filter [19, 20, 21, 22] and the Particle Filter [23] have been effectively implemented. Other solutions have been proposed to increase tracking capabilities, such as the Interactive Multiple Model (IMM) [24, 25], but they are vulnerable to failure when dealing with highly manoeuvrable objects and long-term occlusions.

It is vital to use past information, such as target behaviour, while dealing with such agile and occluded settings. In the prediction stage, the behaviours can be learned and applied. Some researchers have shown that people movements have general patterns in diverse contexts due to constraints on ambient structures and physical motions [26, 27].

The Gaussian Processes (GP) approach was later devised by J. Ko et al [28, 29] to adapt motion patterns and integrate the model in Bayesian Filters. By combining maximum modelling flexibility with uniform uncertainty estimates, GP learns training data for probabilistic regression models. These probabilistic regression models are then used with probabilistic filtering techniques such as the Extended Kalman Filter (EKF) and the Particle Filter (PF) [30, 31, 32].

However, such training data accumulative increment has causing a data management issue which lead towards instability to the learning process of GPs as it occurs in the work done by J. Ko et al [28]. Data redundancies contribute to unnecessary training data which lead to computational intractability due to slight fluctuations and accumulative amount of data. It is not always necessary to maintain all redundant data that does not contribute extra information to the probabilistic regression models. Larger amount of data will increase the computational time to produce the learned GP models. To solve the problem, a technique is proposed that only keeps the most informative data points utilising Mutual Information (MI) [33] and Mahalanobis Distance (MD) [34] criteria.

Due to data redundancy, this work implemented data selection and management in GP, and finally a comparison of four tracking techniques: Extended Kalman Filter (EKF), Particle Filter (PF), Gaussian Processes-Extended Kalman Filter (GP-EKF), and Gaussian Processes-Particle Filter (GP-PF) was carried out by looking at the performance of tracking capabilities towards moving targets and occluded scenarios. The visual and analytical tracking precision of GP-BayesFilters has been compared to the Conventional Bayesian Filters.

The structure of this paper is as follows. The data management and selection processes are discussed in Section 2. The details of Gaussian Processes, combination of Gaussian Process - Particle Filter and Gaussian Process - Extended Kalman Filter are presented in Section 3. The experimental settings is explained in Section 4. Section 5 goes into the experimental findings and the three-step optimization techniques used to keep a number of data points. The paper comes to a conclusion with Section 6.

2. Data Selection and Management

All the samples in training phase of the GP need to be included and periodically new samples will be added whenever it is available. However, when accumulative amount of data becomes comparatively in large numbers, it will practically increase the computing time for the GP to be trained in dealing with new observations [35, 36]. In this research, the motion model of people tracking scenario are learned and needed to be adapted timely to accomodate variations of data samples. When additional observations become available, GP must be trained over a larger number of samples. If the samples are informative, however, further observations must be added. A Mutual Information (MI) based method and Mahalanobis Distance (MD) based criterion can be used to choose informative samples. MI selects the most informative measurements from all scans and uses them to represent GP variables.

MD will be computed between the new measurements or observation data points from LiDAR and the GP model when new measurements become available. Because the GP is easily capable of representing the data set, if each of the new measurements is within 95% of the confidence interval, it will be deleted. However, if the MD exceeds the 95% confidence interval in either x or y direction, it must be inserted into the training samples for GP in order to properly reflect the data. This procedure controls data management and adjusts GP variables to new conditions. The process flow on data selection in Gaussian Processes variables is shown in Fig. 1.

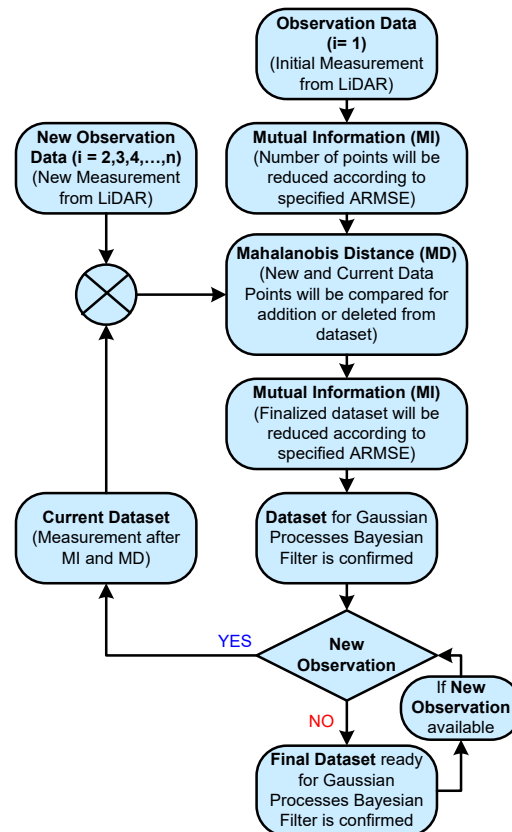


Fig. 1. The process flow on selection of data points in Gaussian Processes.

2.1. Mutual Information

The most informative data points are chosen using the Mutual Information (MI) algorithm [33]. It starts with an empty set of locations $A = \phi$ and adds placement in a sequential order until $|A| = k$. More specifically, the MI algorithm selects the next point with the greatest gain in mutual information. When all k best points have been set in order, the process is complete. The MI between subset A and rest of trajectory $V \setminus A$ can be expressed more precisely as follows [33]:

$$F(A) = I(A; V \setminus A)$$

Once $y \in V \setminus A$ is selected and added to A , the calculation on variation of MI can be done as follows:

$$F(A \cup y) - F(A) = H(A \cup y) - H(A \cup y | \bar{A}) - [H(A) - H(A | \bar{A} \cup y)] = H(y | A) - H(y | \bar{A}) \quad (1)$$

2.2. Mahalanobis Distance

The Mahalanobis Distance (MD) [34] is used to determine the usefulness of new information to be integrated in the GP trained model. This determination, as previously stated, allows the GP to depict dynamically changing environments and consequently increase flexibility.

Assume that a new measurement value of mean μ_{xm} and variance σ_{xm} is obtained at a location \mathbf{x}_i , where $\mathbf{x} = \langle x, y \rangle$. The GP can then be applied to predict the mean μ_{xp} and variance σ_{xp} at the new position of measurement value. As a result, the MD can be written as

$$d(\mathbf{x}) = \sqrt{\frac{(\mu_{xm} - \mu_{xp})^2}{\sigma_{xm}^2 + \sigma_{xp}^2}}. \quad (2)$$

Since the measurement employed for this selection is one-dimensional, the chi-square table criterion for $d(\mathbf{x})$ is set to be within the 95% confidence interval, which is 3.84 [37].

3. Gaussian Process

Gaussian Processes (GP) are a comprehensive theoretical framework for model selection and probability prediction that may be used to explain the uncertainty of complicated data sets. The marginalisation property of Gaussian Processes is an extension of the multivariate Gaussian distribution [38]. Let $D = \langle X, \mathbf{y} \rangle$ be a set of training data, with $X = [\mathbf{x}_1, \mathbf{x}_2, \dots, \mathbf{x}_n]$ a matrix containing d -dimensional input samples and $\mathbf{y} = [y_1, y_2, \dots, y_n]$ a vector containing scalar output. To forecast the regression output, the GP assumes that the data originated from a noisy process with a noisy version of function, $\mathbf{y} = f(\mathbf{x}) + \varepsilon$, where ε is zero mean additive Gaussian noise with σ_n^2 variance.

A GP creates a Gaussian predictive distribution over the output \mathbf{y}_* using training data $D = \langle X, \mathbf{y} \rangle$ and a test input \mathbf{x}_* with mean

$$\text{GP}_\mu(\mathbf{x}_*, D) = \mathbf{k}_*^T [K + \sigma_n^2 I]^{-1} \mathbf{y} \quad (3)$$

and variance

$$\text{GP}_\Sigma(\mathbf{x}_*, D) = k(\mathbf{x}_*, \mathbf{x}_*) - \mathbf{k}_*^T [K + \sigma_n^2 I]^{-1} \mathbf{k}_* \quad (4)$$

where K is the $n \times n$ kernel matrix of training input values $\mathbf{k}[m] = k(\mathbf{x}_*, \mathbf{x}_m)$ and $K[m, n] = k(\mathbf{x}_m, \mathbf{x}_n)$. \mathbf{k}_* is a vector consisting of kernel values between the test input \mathbf{x}_* and the training inputs \mathbf{x} . The variance GP_Σ , which is a process noise-dependent uncertainty prediction; and the correlation between the testing and training data. The squared exponential function is a kernel function that is often utilised, is then chosen for this process as given by,

$$k(\mathbf{x}, \mathbf{x}') = \sigma_f^2 e^{-\frac{1}{2}(\mathbf{x} - \mathbf{x}')^T W (\mathbf{x} - \mathbf{x}')^T} \quad (5)$$

where W is a diagonal matrix that contains the length scales for each input dimension. σ_f^2 is the signal variance.

3.1. Gaussian Process Regression

The process noise and the kernel function which are commonly called as hyperparameters in Gaussian Processes (GP) are determined by using numerical optimization techniques like conjugate gradient descent to maximise the log-likelihood of the training data [38]. Consider a d -dimensional trajectory V with the number of points $|V|$. Based on the GP model, value can be predicted at any point $y \in V \setminus A$ if a set of points $A \subset V$ is observed. Let Z_A be a set of values at the finite set A , and z_y be a value at y . The conditional distribution is derived in probabilistic terms at a predicted point of y where Z_A is given as follows [28]:

$$\mu_{y|A} = \mu_y + \Sigma_{yA} \Sigma_{AA}^{-1} (Z_A - \mu_A) \quad (6)$$

$$\sigma_{y|A}^2 = k(y, y) - \Sigma_{yA} \Sigma_{AA}^{-1} \Sigma_{Ay} \quad (7)$$

where Σ_{yA} is a covariance vector with one input for each $\mathbf{x} \in A$ with value $k(y, \mathbf{x})$; Σ_{AA}^{-1} is a covariance matrix of Z_A with each input calculated by $k(\mathbf{x}, \mathbf{x})$; $\mu_{y|A}$ and $\sigma_{y|A}^2$ are conditional mean and variance at y and μ_A is a mean vector of Z_A .

3.2. Gaussian Processes - Particle Filter

The particle filter (PF) is a technique for handling non-linearity in dynamics and measurements that uses approximation. The difficulty of learning process on prediction and observation models that is required by particle filters can be solved using Gaussian process regression. Processes are limited to training prediction models on static observations because learning with a dynamic observer is quite challenging. The state and control, $(\mathbf{x}_k, \mathbf{u}_k)$, are mapped to the state transition, $\Delta\mathbf{x}_k = \mathbf{x}_{k+1} - \mathbf{x}_k$. By simply adding the state transitions to the preceding state, succeeding state of the process model can be found. The data sets for prediction and observation training are adequately exemplified by,

$$D_p = \langle (X, U), X' \rangle \quad (8)$$

where X is a matrix containing locations and $X' = [\Delta x_1, \Delta x_2, \dots, \Delta x_k]$ is a matrix containing transitions made from those states when employing the controls that stored in U .

$$p(\mathbf{x}_k | \mathbf{x}_{k-1}, \mathbf{u}_{k-1}) \approx N(\text{GP}_\mu([x_{k-1}, \mathbf{u}_{k-1}], D_p), \text{GP}_\Sigma([x_{k-1}, \mathbf{u}_{k-1}], D_p)) \quad (9)$$

Representing posteriors over the state \mathbf{x}_k is a primary task of particle filter by setting X_k of weighted samples $X_k = \{\langle \mathbf{x}_k^m, w_k^{(m)} \rangle | m = 1, \dots, M\}$. Here, each \mathbf{x}_k^m is a sample and each $w_k^{(m)}$ is a non-negative numerical factor which called importance weight. This term, $\text{GP}([x_{k-1}, \mathbf{u}_{k-1}], D_p)$ is the short form of the Gaussian represented by $(\text{GP}_\mu([x_{k-1}, \mathbf{u}_{k-1}], D_p), \text{GP}_\Sigma([x_{k-1}, \mathbf{u}_{k-1}], D_p))$.

By taking into account the local density of training data, the covariance of this prediction is generally different for each sample. The entire procedure can be found in [28].

3.3. Gaussian Processes - Extended Kalman Filter

An incorporation of GP models into the EKF requires a linearization of the GP function which follows the interpretation that was specified by A. Girard et al [39] besides utilising GP mean and covariance. The derivative of GP mean function for each output dimension can be described as:

$$\frac{\delta(\text{GP}_\mu)(x_*, D)}{\delta(x_*)} = \frac{\delta(\mathbf{k}_*)^T}{\delta(x_*)} [K + \delta_n^2 I] y. \quad (10)$$

Noted that \mathbf{k}_* is the vector of kernel values between query input x_* and the training inputs X . The partial derivatives of the kernel vector function are

$$\frac{\delta(\mathbf{k}_*)}{\delta(x_*)} = \begin{bmatrix} \frac{\delta(k(x_*, x_1))}{\delta(x_*[1])} & \dots & \frac{\delta(k(x_*, x_1))}{\delta(x_*[d])} \\ \vdots & \ddots & \vdots \\ \frac{\delta(k(x_*, x_n))}{\delta(x_*[1])} & \dots & \frac{\delta(k(x_*, x_n))}{\delta(x_*[d])} \end{bmatrix}. \quad (11)$$

where d is the dimensionality of input space and n is the number of training points. The partial derivatives are depend on the type of kernel function. For the squared exponential kernel, the expression will be as:

$$\frac{\delta(k(x_*, x))}{\delta(x_*[i])} = -W_{ii} \sigma_f^2 (x_*[i] - x[i]) \exp^{-\frac{1}{2}(x_* - x)W(x_* - x)^T}. \quad (12)$$

Stacking l Jacobian vectors together can determine full $l \times d$ Jacobian of a prediction or observation model which is one for each of the output dimensions. Comprehensive explanation can be found in [28].



Fig. 2. Common area of the research centre.

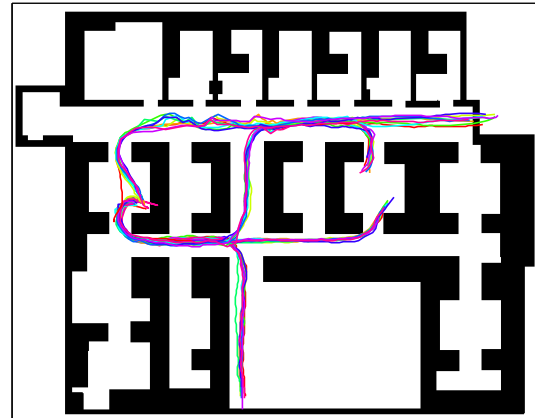


Fig. 3. Routes of walking person on a horizontal map.

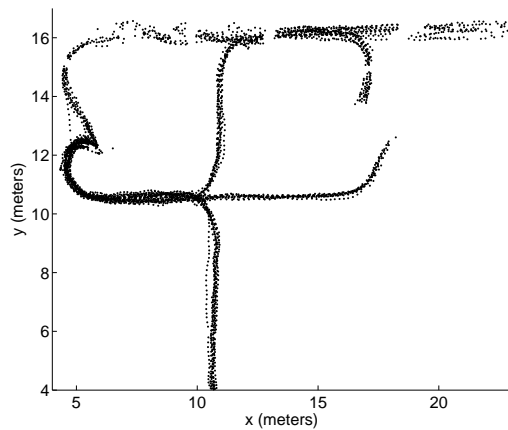


Fig. 4. 3868 dots represents trajectories of the subject.

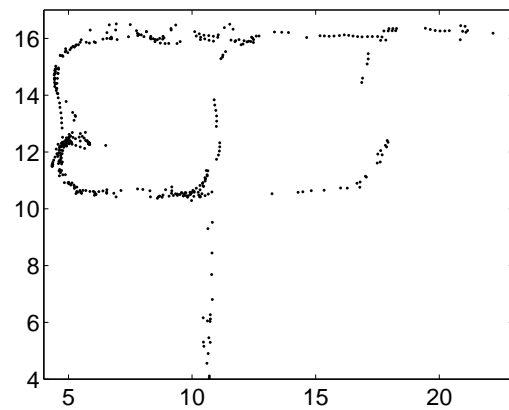


Fig. 5. 381 points in four routes after applying MI and MD.

4. Experiment Scenario

The Segway robot with a laser range finder and a computer was employed as the platform. This system employs a HOKUYO UTM-30LX LiDAR with a detection range of 30 metres, an angular resolution of 0.25° , a field of view coverage of 270° , and a sampling period of 25 milliseconds. The observation of targets is carried out in a stationary posture or a static position to scan the environment horizontally. As indicated in Fig. 2, the experiments were conducted in a common area of research centre.

The method for detecting humans is conducted on laser data taken at torso height of an adult. It starts with features extraction and then proceeds on to a classification process utilising a learning algorithm [40]. Following the detection of people and their representation as points in Cartesian coordinates based on laser data, all of these points were employed in GP modelling. A person was used as a subject in the experiment, who walked many times in four different directions while being observed by the laser sensor. Fig. 3 shows a trace of such trajectories with ten routes in one direction.

Since the width of walking paths between the partitions varies between 130 and 150cm, the main objective is maintaining the RMSE on the prediction below 5 cm. The EKF, PF, GP-PF and GP-EKF will eventually be utilised as a tool for tracking people. Whilst, the performance of GP-EKF and GP-PF are then compared to EKF and PF.

5. Experimental Results

In order to accomplish the optimisation task, the training data was processed in three phases. First step, MI is used to calculate the least number of points that can representing the GPs with the specified average root mean square error on the first set of data in the trajectory. Second, each new measurement is subjected to the MD to ensure that it contributes to new knowledge. Finally, the MI is again used to delete any redundant data points that have arisen as a result on the addition of new data. This process will recursively implemented until it reaches the set value of ARMSE.

This figures show that Fig. 4 shows 3868 points (each representing a person) collected along 10 trajectories of four different routes. The observation's starting point is at coordinate (10, 10). When a set of new samples for the training data became available, MD was used to compare the predicted and measured of mean and covariance values on each point in the x and y axes. The points with an MD of less than 3.84 in either x or y direction (as determined by the chi square table) were deleted. For example, the majority of new data in Fig. 6 provide less MDs than the learned model's threshold, hence the data which values below the threshold were removed. Fig. 8 and Fig. 10 depict the learned GP model means and covariances before applying MI and MD, respectively. Fig. 9 and Fig. 11 depict the learned GP model means and covariances after applying MI and MD, respectively.

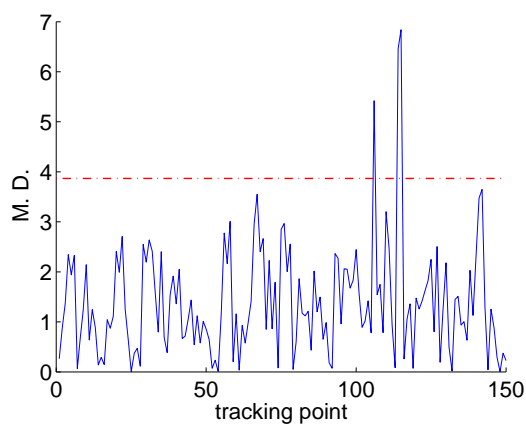


Fig. 6. Mahalanobis Distance in the x direction.

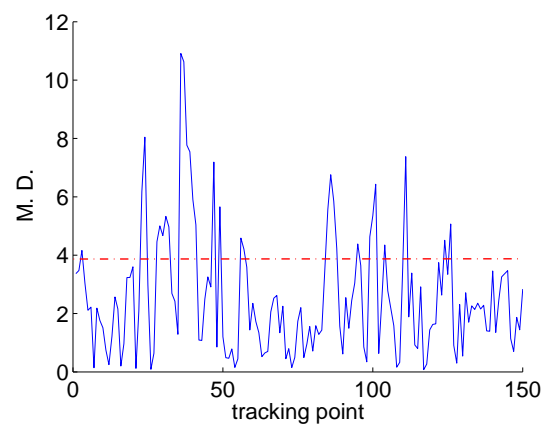


Fig. 7. Mahalanobis Distance in the y direction.

Less MDs indicate that the data are assumed to have been represented in the GP model and hence contribute no further information to the present model. The data was then processed using MI-based data selection to produce a set of points representing the previously determined RMSE of 5 cm. However, as seen in Fig. 6 and Fig. 7, additional data variations resulted in MDs that were greater than the threshold. For retraining purposes, such points were subsequently added into the training samples.

Once the data to be included in the model was determined using MD, MI was used to pick the most informative data points, as illustrated in Fig. 5. The mean and covariance after retraining are shown in Fig. 9 and Fig. 11, and it can be seen that most of the data on predicted mean have RMSE of less than 0.02 metre as shown in Fig. 12. It is seen that the GP predictions will be very close to zeroing values near the corners of 3D-plot where no observations were made.

Referring to Fig. 4 and Fig. 5, the number of training data points was decreased from 3868 points to 381 points, resulting in a data reduction of more than 90 percent.

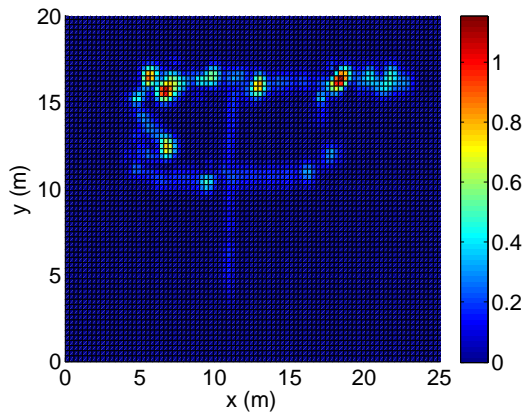


Fig. 8. Mean Values before applying MI and MD.

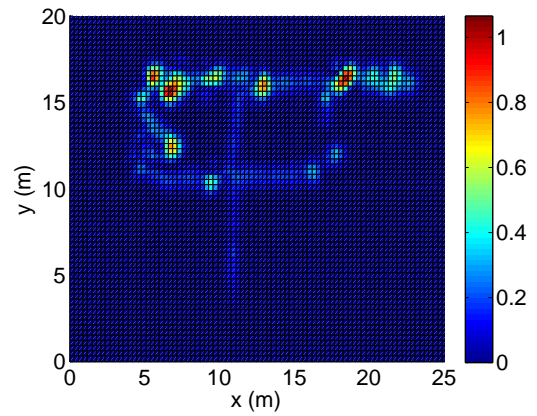


Fig. 9. Mean Values after applying MI and MD.

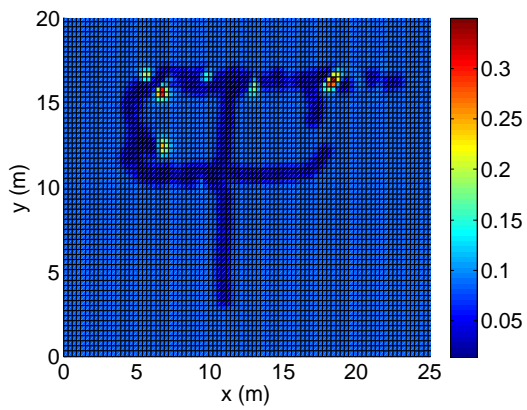


Fig. 10. Covariance Values before applying MI and MD.

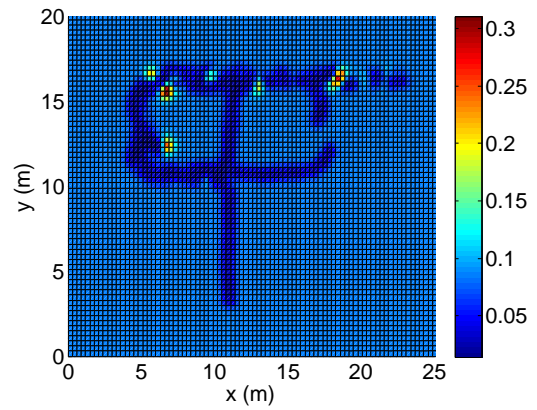


Fig. 11. Covariance Values after applying MI and MD.

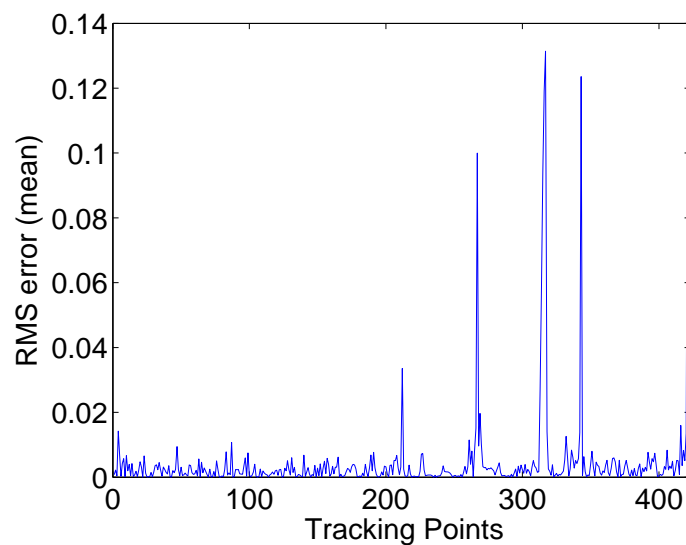


Fig. 12. RMS Error of the Predicted Mean.

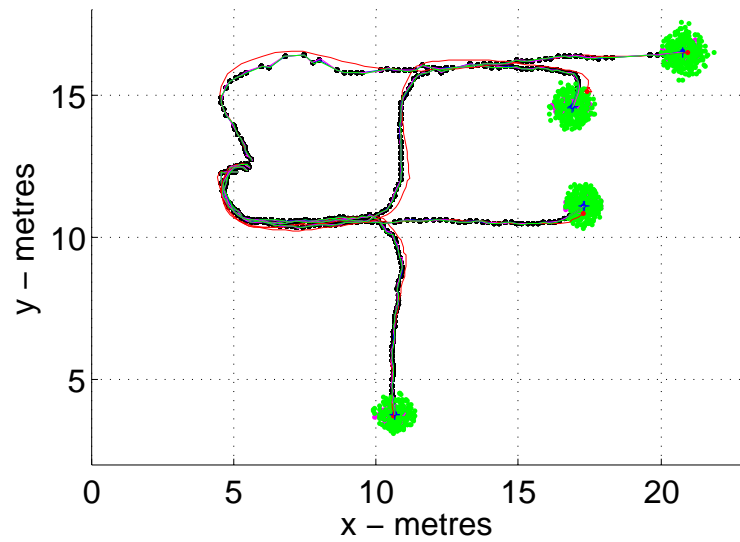


Fig. 13. Tracking on 4 routes without occlusions by EKF (red line), PF (magenta line), GP-EKF (blue line), GP-PF (green line) and black dots represent routes' reference points or ground truth.

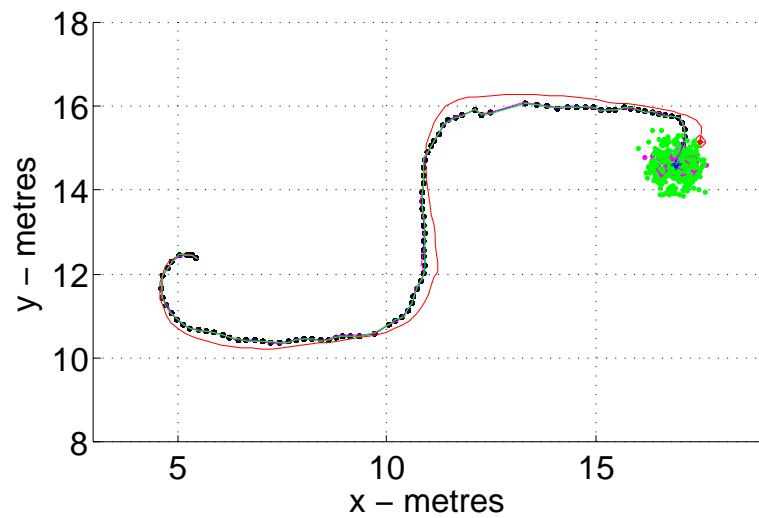


Fig. 14. Tracking on 1 route without occlusions by EKF (red line), PF (magenta line), GP-EKF (blue line) and GP-PF (green line) and black dots represent routes' reference points or ground truth.

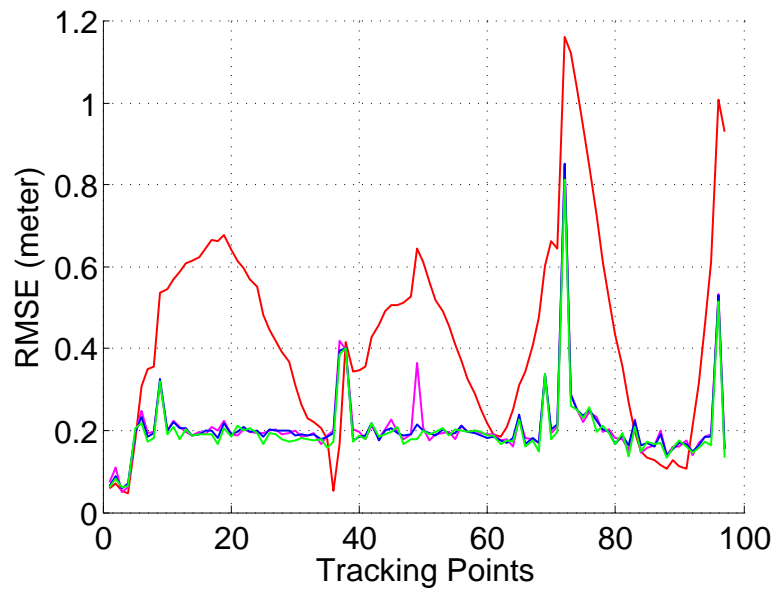


Fig. 15. Comparison of RMS Error on 1 route without occlusions for tracking by EKF (red line), PF (magenta line), GP-EKF (blue line) and GP-PF (green line).

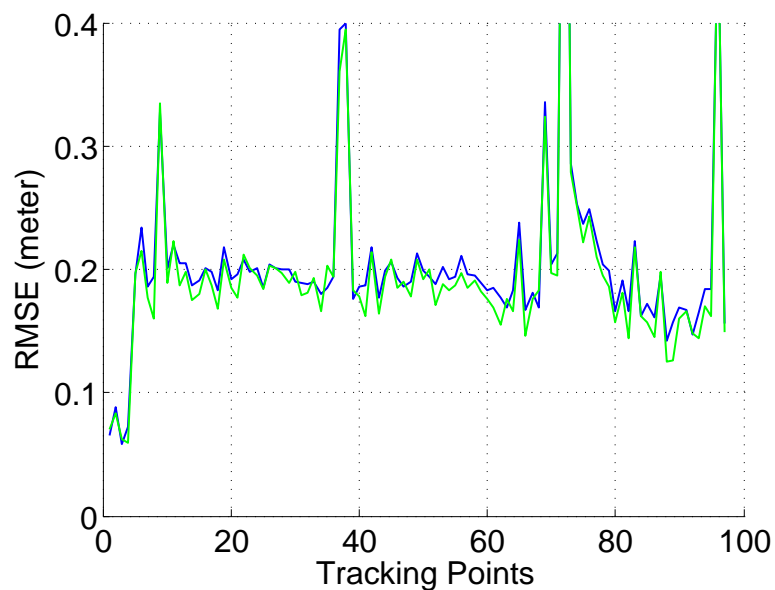


Fig. 16. Comparison of RMS Error on 1 route without occlusions for tracking by GP-EKF (blue line) and GP-PF (green line).

People are tracked on four routes at the same time without any occlusion in Fig. 13. GP-PF, GP-EKF, EKF, and PF trackers are represented by green, blue, red, and magenta lines, respectively. The black dots represent the routes' reference points or ground truth. When it comes to manoeuvring conditions, EKF performs the worst among the 4 tracking methods. By comparing the RMSE on

50 Monte Carlo runs as shown in Fig. 15, a study of each tracker's performance at only one route as shown in Fig. 14 was performed. As referred to Table 1, GP-PF and GP-EKF have convincingly demonstrated that they have greater tracking performance than EKF and PF because of their lower ARMSE. Table 2 shows the tracking points with RMSE value less than 0.25 meters which proved that GP-EKF and GP-PF have the higher number of points. The comparison on only GP-PF and GP-EKF trackers in Fig. 16 shows that GP-PF performs marginally better than GP-EKF because GP-PF has a lower RMSE than GP-EKF.

Table 1. Average Root Mean Square Error (ARMSE) for EKF, PF, GP-EKF and GP-PF trackers in Fig. 15.

Type of Tracker	EKF	PF	GP-EKF	GP-PF
ARMSE (meter)	0.4326	0.2094	0.2059	0.1986

Table 2. Tracking points with RMSE less than 0.25 meters for EKF, PF, GP-EKF and GP-PF trackers in Fig. 15.

Type of Tracker	EKF	PF	GP-EKF	GP-PF
No. of Points \leq 0.25 meter	25	87	88	90
(Total Points is 97)				

The simultaneous tracking of four paths with partial occlusion where there were no observation data on particular frames by GP-PF and GP-EKF trackers is shown in Fig. 17. With a specific period of time, both trackers have demonstrated greater tracking performance on occlusions. The tracking performance of four trackers on four routes with partial occlusions is shown in Fig. 18. It has been demonstrated that both Conventional Bayesian Filters (PF and EKF) perform badly when compared to Gaussian Process-BayesFilters (GP-PF and GP-EKF), where both Conventional Bayesian Filters perform poorly on tracking with partial occlusions over time.

6. Conclusion and Future Work

In this study, a MI and MD-based criterion for rejecting least informative data points was effectively adopted while quickly training a GP model for tracking multiple people in a fairly complicated indoor setting. The proposed approach reduced data points up to more than 90% while keeping the ARMSE within acceptable limits. This is a promising data optimization that will help reducing computational time, especially when deal with periodic accumulative data set. The learned GP which incorporated with Bayesian Filters was then used to track people along the different paths in the vicinity. When compared to PF and EKF trackers, both GP-PF and GP-EKF have achieved higher tracking performance when dealing with occlusions. When comparing both Gaussian Process-BayesFilters, GP-PF fared slightly better than GP-EKF. Furthermore, the performance of Gaussian Process-BayesFilters is not affected by walking speed of people since state transitions are based on displacements in x and y coordinates. However, Gaussian Process model need to be trained for specific environment and different scenarios.

In the future, this technique will be evaluated on various scenarios involving numerous sub-sectors for broad coverage area because too many data points will increase computational time. Thus, dividing a big area into smaller areas saves computing time.

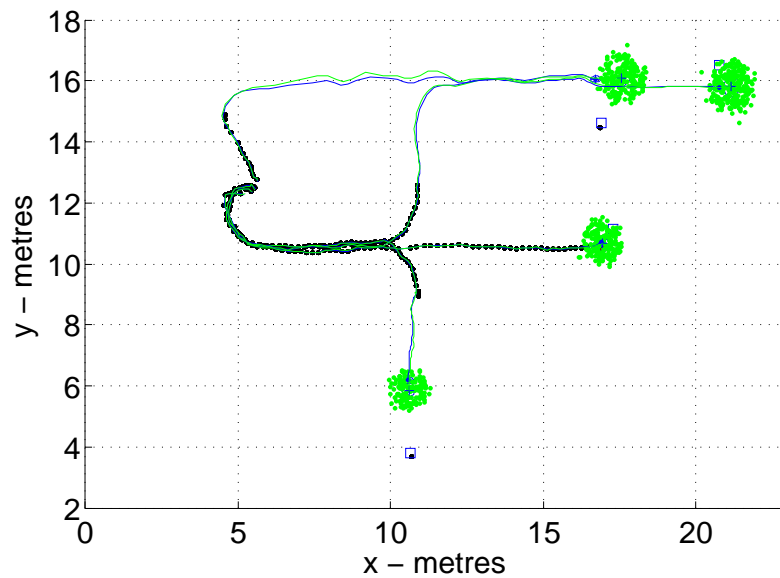


Fig. 17. Tracking comparison with partial occlusion by using GP-PF (green), GP-EKF (blue line) and black dots represent routes' reference points or ground truth.

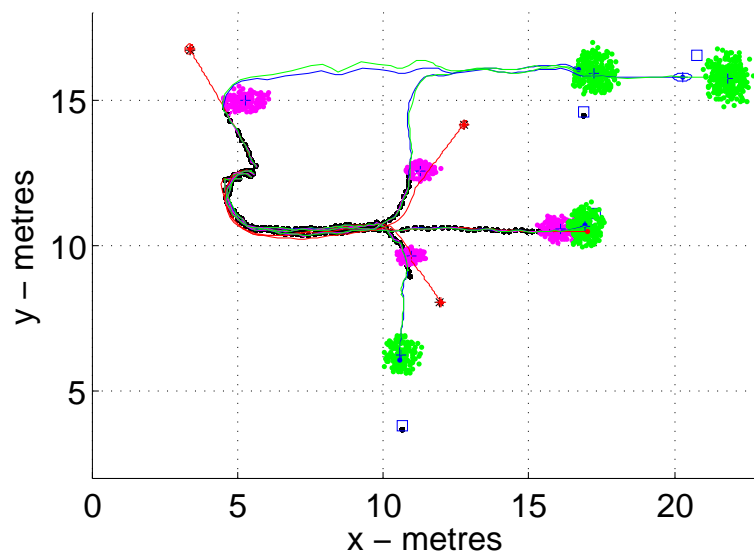


Fig. 18. Tracking with partial occlusion by EKF (red line), PF (magenta line), GP-EKF (blue line), GP-PF (green line) and black dots represent routes' reference points or ground truth.

Author Contribution: All authors contributed equally to the main contributor to this paper. All authors read and approved the final paper.

Funding: This work is supported by the Centre of Autonomous Systems (CAS), University of Technology, Sydney, Australia; Centre for Telecommunication Research and Innovation (CeTRI), Universiti Teknikal Malaysia Melaka (UTeM), Malaysia and the Ministry of Higher Education (MoHE), Malaysia.

Acknowledgment: The author would like to thank to Centre of Autonomous Systems (CAS), University of Technology, Sydney, Australia; Centre for Telecommunication Research and Innovation (CeTRI), Universiti Teknikal Malaysia Melaka (UTeM), Malaysia and the Ministry of Higher Education (MoHE), Malaysia for research funding.

Conflicts of Interest: The authors declare no conflict of interest.

References

- [1] K. Koide, J. Miura, and E. Menegatti, "Monocular person tracking and identification with on-line deep feature selection for person following robots," *Robotics and Autonomous Systems*, vol. 124, p. 103348, 2020, <https://doi.org/10.1016/j.robot.2019.103348>.
- [2] J. Alberts, S. Kleinschmidt, and B. Wagner, "Robust calibration procedure of a manipulator and a 2d laser scanner using a 1d calibration target," in *17th International Conference on Informatics in Control, Automation and Robotics*, 2019, <https://www.scitepress.org/Papers/2019/79467/79467.pdf>.
- [3] A. H. A. Rahman, K. A. Z. Ariffin, N. S. Sani, and H. Zamzuri, "Pedestrian detection using triple laser range finders," *International Journal of Electrical & Computer Engineering*, vol. 7, no. 6, 2017, <http://doi.org/10.11591/ijece.v7i6.pp3037-3045>.
- [4] H. Beomsoo, A. A. Ravankar, and T. Emaru, "Mobile robot navigation based on deep reinforcement learning with 2d-lidar sensor using stochastic approach," in *2021 IEEE International Conference on Intelligence and Safety for Robotics (ISR)*, 2021, <https://doi.org/10.1109/ISR50024.2021.9419565>.
- [5] N. Tsoulias, G. Xanthopoulos, S. Fountas, and M. Zude, "In-situ detection of apple fruit using a 2d lidar laser scanner," in *2020 IEEE International Workshop on Metrology for Agriculture and Forestry (MetroAgriFor)*, 2020, <https://doi.org/10.1109/MetroAgriFor50201.2020.9277629>.
- [6] J. Chen, P. Ye, and Z. Sun, "Pedestrian detection and tracking based on 2d lidar," *The 2019 6th International Conference on Systems and Informatics (ICSAI 2019)*, pp. 421–426, 2019, <https://doi.org/10.1109/ICSAI48974.2019.9010202>.
- [7] L. Beyer, A. Hermans, T. Linder, K. O. Arras, and B. Leibe, "Deep person detection in two-dimensional range data," *IEEE Robotics and Automation Letters*, vol. 3, pp. 2726–2733, 2018, <https://doi.org/10.1109/LRA.2018.2835510>.
- [8] S. Chan, R. E. Warburton, G. Garipey, J. Leach, and D. Faccio, "Non-line-of-sight tracking of people at long range," *Optic Express*, vol. 25, no. 9, pp. 10 109–10 117, 2017, <https://doi.org/10.1364/OE.25.010109>.
- [9] A. Borcs, B. Nagy, and C. Benedek, "Instant object detection in lidar point clouds," *IEEE Geoscience and Remote Sensing Letters*, pp. 992–996, 2017, <https://doi.org/10.1109/LGRS.2017.2674799>.
- [10] Y. Li and J. Ibañez-Guzmán, "Lidar for autonomous driving: The principles, challenges, and trends for automotive lidar and perception systems," *IEEE Signal Process. Mag.*, vol. 37, no. 4, pp. 50–61, 2020, <https://doi.org/10.1109/MSP.2020.2973615>.
- [11] Y. Nakamori, Y. Hiroi, and A. Ito, "Multiple player detection and tracking method using a laser range finder for a robot that plays with human," *ROBOMECH Journal*, vol. 5, no. 1, pp. 1–15, 9 2018, <https://doi.org/10.1186/s40648-018-0122-x>.
- [12] D. Gruyer and M.-C. Rahal, "Multi-layer laser scanner strategy for obstacle detection and tracking," in *2019 IEEE/ACS 16th International Conference on Computer Systems and Applications (AICCSA)*, 2019, <https://doi.org/10.1109/AICCSA47632.2019.9035243>.

-
- [13] M. E. Warren, "Automotive lidar technology," in *2019 Symposium on VLSI Circuits*, 2019, pp. C254–C255, <https://doi.org/10.23919/VLSIC.2019.8777993>.
- [14] D. Katkoria and J. Sreevalsan-Nair, "Rosels: Road surface extraction for 3d automotive lidar point cloud sequence," in *Proceedings of the 3rd International Conference on Deep Learning Theory and Applications - DeLTA*, 2022, pp. 55–67, <https://www.scitepress.org/PublishedPapers/2022/113017/113017.pdf>.
- [15] Z. Dai, A. Wolf, P. Ley, T. Glück, M. C. Sundermeier, and R. Lachmayer, "Requirements for automotive lidar systems," *Sensors*, vol. 22, no. 19, p. 7532, 2022, <https://doi.org/10.3390/s22197532>.
- [16] V. L. Popov, S. A. Ahmed, N. G. Shakev, and A. V. Topalov, "Detection and following of moving targets by an indoor mobile robot using microsoft kinect and 2d lidar data," in *2018 15th International Conference on Control, Automation, Robotics and Vision (ICARCV)*, 2018, pp. 280–285, <https://doi.org/10.1109/ICARCV.2018.8581231>.
- [17] M. L. Simpson and D. P. Hutchinson, "Imaging — lidar," in *Encyclopedia of Modern Optics*, R. D. Guenther, Ed. Oxford: Elsevier, 2005, pp. 169–178, <https://doi.org/10.1016/B0-12-369395-0/00720-X>.
- [18] P. Dong and Q. Chen, *LiDAR Remote Sensing and Applications*. CRC Press, 2018, <https://doi.org/10.4324/9781351233354>.
- [19] S. Bhaumik and P. Date, *The Kalman filter and the extended Kalman filter*. Chapman and Hall/CRC, 2019, ch. Book: Nonlinear Estimation, pp. 27–50, <http://dx.doi.org/10.1201/9781351012355-2>.
- [20] D. Schulz, W. Burgard, D. Fox, and A. B. Cremers, "People tracking with mobile robots using sample-based joint probabilistic data association filters," *International Journal of Robotics Research*, vol. 22, no. 2, pp. 99–116, 2003, <https://doi.org/10.1177/0278364903022002002>.
- [21] I. Ullah, X. Su, X. Zhang, and D. Choi, "Simultaneous localization and mapping based on kalman filter and extended kalman filter," *Wirel. Commun. Mob. Comput.*, vol. 2020, pp. 1–12, 2020, <https://doi.org/10.1155/2020/2138643>.
- [22] A. Roux, S. Changey, J. Weber, and J.-P. Lauffenburger, "Projectile trajectory estimation: performance analysis of an extended kalman filter and an imperfect invariant extended kalman filter," in *2021 9th International Conference on Systems and Control (ICSC)*, 2021, <https://doi.org/10.1109/ICSC50472.2021.9666713>.
- [23] D. Schulz, D. Fox, and J. Hightower, "People tracking with anonymous and id-sensors using rao-blackwellised particle filters," in *Proceedings of the 18th international joint conference on Artificial intelligence*, 2003, pp. 921–928, <https://dl.acm.org/doi/10.5555/1630659.1630792>.
- [24] B. Kovacevic, D. Ivkovic, and Z. Radosavljevic, "Immpdaf approach for l-band radar multiple target tracking," in *2020 19th International Symposium INFOTEH-JAHORINA (INFOTEH)*, 2020, pp. 1–5, <https://doi.org/10.1109/INFOTEH48170.2020.9066328>.
- [25] K. R. S. Kodagoda, S. S. Ge, W. S. Wijesoma, and A. P. Balasuriya, "Immpdaf approach for road-boundary tracking," *IEEE Transactions on Vehicular Technology*, vol. 56, no. 2, pp. 478–486, 2007, <https://doi.org/10.1109/TVT.2007.891426>.
- [26] A. Escobedo, A. Spalanzani, C. Laugier *et al.*, "Experimental setup for human aware navigation," in *Control Architectures of Robots*, 2012, <http://hal.inria.fr/hal-00746567/>.
- [27] S. Morishita, A. Nishimura, and H. Asama, "A method to estimate destination of a walking person with hidden markov model for safety of human friendly robots," in *Safety, Security and Rescue Robotics, 2008. SSRR 2008. IEEE International Workshop on*, 2008, pp. 115–120, <https://doi.org/10.1109/SSRR.2008.4745887>.
- [28] J. Ko and D. Fox, "Gp-bayesfilters: Bayesian filtering using gaussian process prediction and observation models," *Autonomous Robots*, vol. 27, no. 1, pp. 75–90, 2009, <https://doi.org/10.1007/s10514-009-9119-x>.
- [29] J. Ko and D. Fox, "Gp-bayesfilters: Bayesian filtering using gaussian process prediction and observation models," in *2008 IEEE/RSJ International Conference on Intelligent Robots and Systems*, 2008, <https://doi.org/10.1109/iros.2008.4651188>.

-
- [30] C. Plagemann, D. Fox, and W. Burgard, "Efficient failure detection on mobile robots using particle filters with gaussian process proposals," in *Proc. of the Twentieth International Joint Conference on Artificial Intelligence (IJCAI)*, 2007, <https://dl.acm.org/doi/10.5555/1625275.1625628>.
- [31] A. Fod, A. Howard, and M. Mataric, "A laser-based people tracker," in *Proceedings. ICRA'02. IEEE International Conference on Robotics and Automation, 2002.*, vol. 3, 2002, pp. 3024–3029, <https://doi.org/10.1109/ROBOT.2002.1013691>.
- [32] M. F. Bugallo, S. Xu, and P. M. Djuric, "Comparison of ekf- and pf-based methods in tracking maneuvering targets," in *2006 IEEE Aerospace Conference*, 2006, <https://doi.org/10.1109/AERO.2006.1655921>.
- [33] C. Guestrin, A. Krause, and A. Singh, "Near-optimal sensor placements in gaussian processes," in *Proceedings of the 22nd international conference on Machine learning*, 2005, pp. 265–272, <https://doi.org/10.1145/1102351.1102385>.
- [34] R. De Maesschalck, D. Jouan-Rimbaud, and D. L. Massart, "The mahalanobis distance," *Chemo-metrics and Intelligent Laboratory Systems*, vol. 50, no. 1, pp. 1–18, 2000, [https://doi.org/10.1016/S0169-7439\(99\)00047-7](https://doi.org/10.1016/S0169-7439(99)00047-7).
- [35] Z. Zainudin, M. M. Ibrahim, and S. Kodagoda, "Non-parametric data optimization for 2d laser based people tracking," in *12th IEEE Conference on Industrial Electronics and Applications (ICIEA)*, 2017, pp. 1887–1892, <https://doi.org/10.1109/ICIEA.2017.8283146>.
- [36] Z. Zainudin, S. Kodagoda, and G. Dissanayake, "Mutual information based data selection in gaussian processes for 2d laser range finder based people tracking," in *2013 IEEE/ASME International Conference on Advanced Intelligent Mechatronics*, 2013, pp. 477–482, <https://doi.org/10.1109/AIM.2013.6584137>.
- [37] G. Schay, *Introduction to probability with statistical applications*. Birkhäuser, 2007, <https://doi.org/10.1007/978-3-319-30620-9>.
- [38] C. E. Rasmussen and C. K. I. Williams, *Gaussian processes for machine learning*. MIT press Cambridge, 2006, <https://books.google.co.id/books?id=Tr34DwAAQBAJ>.
- [39] A. Girard, C. E. Rasmussen, J. Q. Candela, and R. Murray-Smith, "Gaussian process priors with uncertain inputs - application to multiple-step ahead time series forecasting," in *Advances in Neural Information Processing Systems*, 2002, pp. 529–536, <https://proceedings.neurips.cc/paper/2002/hash/f3ac63c91272f19ce97c7397825cc15f-Abstract.html>.
- [40] Z. Zainudin, S. Kodagoda, and G. Dissanayake, "Torso detection and tracking using a 2d laser range finder," in *Proceedings of the Australasian Conference on Robotics and Automation*, 2010, <http://hdl.handle.net/10453/16405>.